Jurnal
Teknologi

Full Paper

SENSITIVITY MAPS RECONSTRUCTION FOR MAGNETIC INDUCTION TOMOGRAPHY MODALITY USING EXPERIMENTAL TECHNIQUE

Zulkarnay Zakaria[a*], Hafizi Suki[a], Masturah Tunnur Mohamad Talib[a], Ibrahim Balkhis[a], Maliki Ibrahim[a,b], Muhammad Saiful Badri Mansor[c], Mohd Hafiz Fazalul Rahiman[a], Ruzairi Abdul Rahim[c]

[a]Tomography Imaging Research Group, School of Mechatronic Engineering, Universiti Malaysia Perlis, 02600 Arau, Perlis, Malaysia
[b]School of Manufaturing Engineering, Universiti Malaysia Perlis, 02600 Arau, Perlis, Malaysia
[c]Process Tomography and Instrumentation Engineering Research Group (PROTOM-i), Faculty of Electrical Engineering, UniversitiTeknologi Malaysia, 81310, UTM Johor Bahru, Johor Malaysia

Article history
Received
28 June 2015
Received in revised form
1 September 2015
Accepted
15 October 2015

*Corresponding author
zulkarnay@unimap.edu.my

Graphical abstract

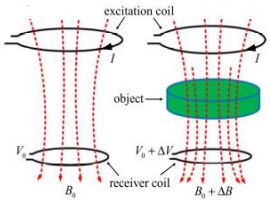

Abstract

Magnetic induction tomography (MIT) is a relatively new non-contacting technique for visualization of passive electrical property distribution inside a media. In any tomography system, the image is reconstructed using image reconstruction algorithm which requires sensitivity maps. There are three methods of acquiring sensitivity maps; finite element technique, analytically or experimentally. This research will focus on the experimentally method. Normally sensitivity map is generates using finite element technique that usually ignore certain parameters in real setup which in turn contribute to errors or blur in the reconstructed image. Thus experimental technique needs to be explored as an improvement as it is based on real parameters exists in the experimental setup. This paper starts with general view of magnetic induction tomography, image reconstruction algorithm and finally on the experimental technique of generating sensitivity maps.

Keywords: Magnetic induction tomography, sensitivity maps, experimental technique

1.0 INTRODUCTION

The principle of Magnetic Induction Tomography (MIT) is based on the mutual inductance theory and the eddy current problem. MIT system is mainly consisted the measuring space that includes of an excitation coil (Tx), detection coil (Rx), transceiver circuits, post processing circuit and data acquisition card to measure the data and transfers the data to the computer and as a result as shown in Figure 1 [1].

In MIT system, an eddy current is induced in the sensor array after generating a magnetic field by the excitation coil. Then, the detection coil senses the eddy current by means of mutual inductance tomography. Magnetic fields generated by using one or more excitation coils to generates an eddy current field within the conductive object material, which in turn produces a secondary magnetic field that can be detected by the sensing coils as shown in Figure 2.

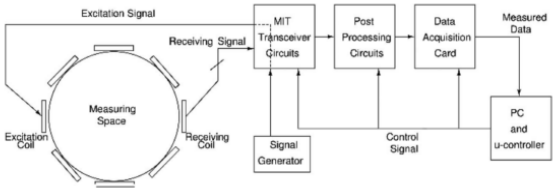

Figure 1 A complete MIT system block diagram [1]

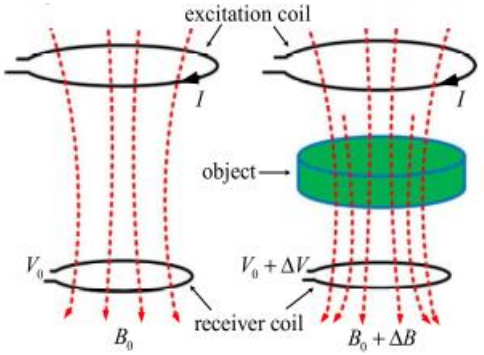

Figure 2 Schematic diagram for principle of MIT [3]

2.0 IMAGE RECONSTRUCTION ALGORITHM

Image reconstruction is an important part of a tomography system which involve both forward and inverse problem. Figure 3 shows the illustration of forward and inverse problem of an MIT system.

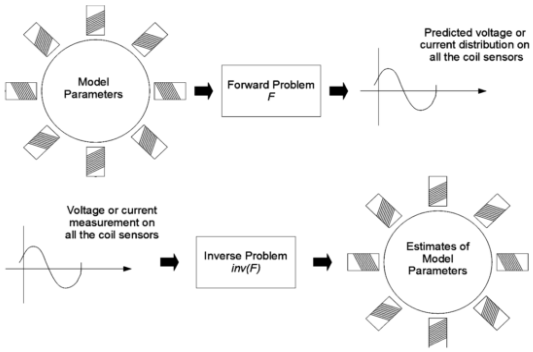

Figure 3 Illustration of forward and inverse problem in MIT[4]

A. Forward Problem

The forward problem of MIT is actually solving a problem of open boundary time-harmonic eddy current field. Assume time-harmonic field, with angular frequency, ω. All the coefficients in equation[1] are expressed as follows.

$$\nabla \times \frac{B}{\mu_0} = \sigma E + J_S \quad (1)$$

$$\nabla \times E = -J\omega B \quad (2)$$

$$\nabla . B = 0 \quad (3)$$

$$\nabla . \varepsilon B = 0 \quad (4)$$

Where σ is conductivity, μ_0 is permeability, ε is permittivity, J_s is the source current in excitation coil, ***B*** is the magnetic flux density and ***E*** is the electric field intensity.

The measured value at the receiver is given by

$$V = -\mathrm{J}\omega \oint \boldsymbol{A}.\boldsymbol{d} \quad (5)$$

Where A is vector potential.

B. Inverse Problem

The forward problem is formulated by linear relation and the goal of inversion is to estimate χ from the observed data The least-squares solution is the one that minimizes the quadratic distance between real data and simulated data S_χ[2].

$$\chi = arg \min_{\chi}[(y - s_\chi)^T (y - s_\chi) \quad (6)$$

The potentials around the object were simulated with the linearized model and were a zero mean, Gaussian white noise whose power was adjusted so as to obtain a 20 dB signal-to-noise ratio (SNR). This reconstruction is obviously not satisfactory, and illustrates the typical ill-posed nature of the inversion: a small amount of noise on the data is sufficient to make the solution extremely unstable. In order to obtain a satisfactory behavior , the problem must be regularized, for example through introduction of a priori information on the unknown object[3].

C. Sensitivity Maps

There are three methods of acquiring sensitivity maps; finite element technique, analytically or experimentally[4].

i. Finite Element Method.

The finite element method is a general technique to obtain approximate solutions to boundary value problems. The method involves dividing the domain of the solution into a finite number of simple subdomains, the finite elements, and using variation concepts to obtain an approximate solution over the collection of finite elements[5]. The example of using FEM method is shown in Figure 4.

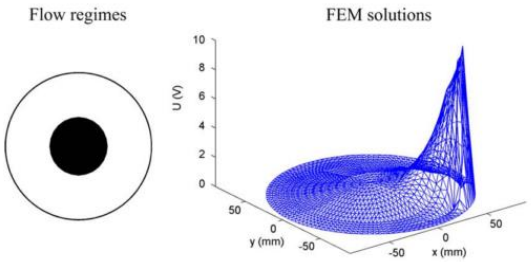

Figure 4 Example of the calculation potential distribution using finite element method[6]

ii. Analytical Method.

In acquiring sensitivity maps, analytical method is among method for solving the sensitivity maps issues. It is done through the use of mathematical equation for predicting system sensitivity as well as testing image reconstruction algorithms[7].

iii. Experimental Method

In the experimental method, there a few techniques can be utilized such as coil arrangements, position of the sample (steel), size and many others[8]. The same measurement method also proposed for subsurface imaging and its potential was shown numerically in three-dimensional (3-D) simulations [9].

3.0 METHODOLOGY

A. Study on MIT Prototype Version 1.0

In the developed MIT measurement system, the jig panels are arranged alternately at equidistance in circular manner as shown in Figure 5. At the receiver coils extraction of the collected data is crucial because receiver coils are sensitive to primary field and interference both from external sources and internal side-by-side coils.To acquire experiment data, the MIT hardware prototype ver 1.0 was used.A 16 channel magnetic induction tomography system was presented.It consists of 8 excitation coil 8 receiving coils. A steel of 1.25 inch diameter is the sample in this experiment. Based on the sample size, there areonly 37 tested positionsavailable for experiment as shown in Figure 6.

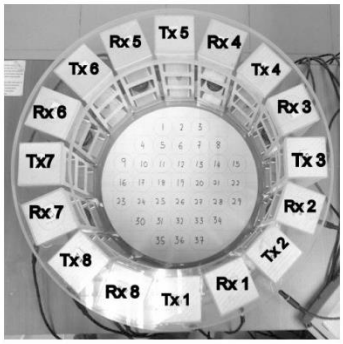

Figure 5 Prototype of MIT ver1.0 measurement system[10]

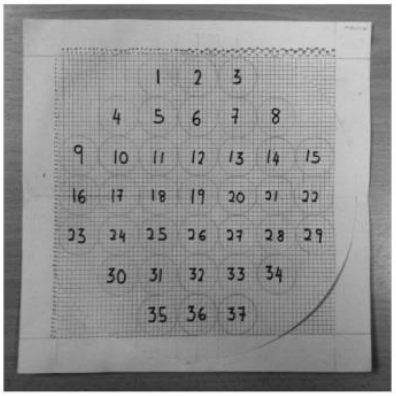

Figure 6 An example of the sample of the position in this experiment

B. ROI Mapping

Functional regions of interest (fROIs) are defined independently in each coil, and those regions are then probed further to determine their precise function.This method was designed to discover regions that are covered systematically across subjects and crucially to define the borders around and between each of these regions.Each voxel in these overlap maps contains information about the number of subjects that have activation in that voxel for a given contrast. Thus, the overlap maps contain information about points of high inter-subject overlap, and also information about the distribution of individual activations around these high overlap points [11]. Figure 6 showsan example of the sample positions in this experiment.

C. Data Collection

There are 64 data in the measurement from 8 transmitter and 8 receiver pairs. In the measurement, there are 2 types of data namely the average value with no object and the average value data with object. An input current of 140 mA at frequency of 500 kHz was fed into the excitation coil with an empty ROI (no sample) and the data was recorded.

Thenmeasurements for with object were taken place starting from the position 1 until position 37.

D. Sensitivity Maps Generation

Data at each position (from position 1- 37) are taken in complete 8 transmitters – 8 receiver measurement scheme which contributed to 64 measurementsin a cycle. Example of measurement for position 1 is shown in Table 1. There are 37 tables should be completed as the positions are 37. These data are normalized using equation (7).

The percentage average of reading value with object is calculated using;

$$\frac{V\ object - V\ no\ object}{V\ no\ object} \times 100 = Percentage\ Average\ of\ object \quad (7)$$

The results as shown in Table 3. To create the sensitivity map of each transmitter-receiver pair, these normalized value from table 1-37 are then map onto the respective transmitter-receiver pair which then produced the sensivity map of that respective pair as shown in Figure 8.

E. Evaluation

Evaluation was done based on the comparison between the generated maps from experimental and FEM.

4.0 RESULT AND DISCUSSION

Examples of average data value with no object and average data value with object is shown in Table 1 and Table 2 respectively.

Table 1 Average data value with no object for position 1

	Rx1	Rx2	Rx3	Rx4	Rx5	Rx6	Rx7	Rx8
Tx1	3.194	2.547	1.129	0.568	0.486	0.815	2.267	3.275
Tx2	2.508	3.823	3.373	0.842	0.464	0.522	0.707	2.305
Tx3	2.263	3.273	4.628	2.67	0.759	0.508	0.482	0.781
Tx4	0.702	2.276	4.494	3.56	2.346	0.805	0.434	0.473
Tx5	0.424	0.742	3.17	3.597	2.968	2.323	0.659	0.47
Tx6	0.458	0.497	1.077	2.689	3.403	3.29	2.134	0.601
Tx7	0.551	0.411	0.564	0.68	1.799	2.644	2.227	1.852
Tx8	2.295	0.813	0.713	0.57	0.793	2.626	3.077	3.352

Table 2 Average data value with object

	Rx1	Rx2	Rx3	Rx4	Rx5	Rx6	Rx7	Rx8
Tx1	3.191	2.547	1.131	0.569	0.463	0.818	2.27	3.275
Tx2	2.509	3.825	3.378	0.848	0.44	0.523	0.708	2.305
Tx3	2.265	3.268	4.625	2.69	0.72	0.505	0.482	0.782
Tx4	0.705	2.282	4.496	3.562	2.294	0.777	0.432	0.474
Tx5	0.423	0.751	3.256	3.646	3.161	2.104	0.622	0.457
Tx6	0.458	0.487	1.022	2.43	3.574	3.315	2.18	0.611
Tx7	0.554	0.411	0.561	0.655	1.813	2.644	2.226	1.854
Tx8	2.296	0.814	0.715	0.565	0.769	2.639	3.075	3.349

Table 3 Percentage Error of Average of scan object

	Rx1	Rx2	Rx3	Rx4	Rx5	Rx6	Rx7	Rx8
Tx1	-0.094	0.000	0.177	0.176	-4.733	0.368	0.132	0.000
Tx2	0.040	0.052	0.148	0.713	-5.172	0.192	0.141	0.000
Tx3	0.088	-0.153	-0.065	0.749	-5.138	-0.591	0.000	0.128
Tx4	0.427	0.264	0.045	0.056	-2.217	-3.478	-0.461	0.211
Tx5	-0.236	1.213	2.713	1.362	6.503	-9.427	-5.615	-2.766
Tx6	0.000	-2.012	-5.107	-9.632	5.025	0.760	2.156	1.664
Tx7	0.544	0.000	-0.532	-3.676	0.778	0.000	-0.045	0.108
Tx8	0.044	0.123	0.281	-0.877	-3.026	0.495	-0.065	-0.089

The sensitivity of each receiver should be any value with the range of positive integer as the activated excitation coil becomes the centre line. Figure 7 shows the generated sensitivity map in relative to the position shown in Figure 5.

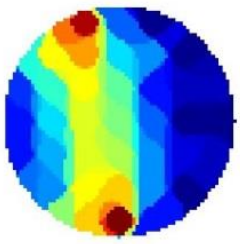

Figure 7 Sensitivity of the receiver coils when Tx1 transmits to the excitation coil Rx5 based on measurement

The generated sensitivity map shows that the agreement between the map and the position arrangement of the prototype. The resolution and accuracy can be improved by using a smaller sample size, thus more locations could be occupied within the ROI.

5.0 CONCLUSION

Generation of sensitivity maps using experimental method proven that this technique could be used in sensitivity maps generation. It is more accurate as the consideration on the real parameters has been taken into account during measurement.

Acknowledgement

The authors would like to thank the Malaysia Government, Universiti Malaysia Perlis (UNIMAP) and Universiti Teknologi Malaysia for funding this research under RACE grant 9017-00175 and Grant Q.J130000.3013.00M52 respectively.

References

[1] Y. Chen, X. Wang, Y. Lv, and D. Yang. 2011. An Image Reconstruction Algorithm Based on Variation Regularization for Magnetic Induction Tomography. In *Cross Strait Quad-Regional Radio Science and Wireless Technology Conference*. 8: 1422-1425.

[2] C. Cohen-bacrie, Y. Goussard, and R. Guardo. 1997. Regularized Reconstruction in Electrical Impedance Tomography Using a Variance Uniformization Constraint. *IEEE*. 16(5): 562-571.

[3] C. Cohen-bacrie, Y. Goussard, and R. Guardo. 1997. Regularized Reconstruction in Electrical Impedance Tomography Using a Variance Uniformization Constraint. *IEEE Trans. Med. Imaging*. 16(5): 562-571.

[4] J. Rosell, R. Casañas, and H. Scharfetter. 2001. Sensitivity Maps And System Requirements For Magnetic Induction Tomography Using A Planar Gradiometer. *Physiol. Meas.* 22(1): 121-130.

[5] J. Juang. Estimation of Solutions to a Second Finite Element Method With Different Boundary Conditions. In *IEEE/ASME International Conference*. 128.

[6] L. Zhang, P. Tian, X. Jin, and W. Tong. 2010. Numerical Simulation Of Forward Problem For Electrical Capacitance Tomography Using Element-Free Galerkin Method. *Eng. Anal. Bound. Elem.* 34(5): 477-482.

[7] H. Griffiths. 2005. Magnetic Induction Tomography. In *Electrical Impedance Tomography: Methods, History and Applications*. 1st Ed. D. S. Holder, Ed. Bristol, UK: Institute of Physics Publishing. 213-238.

[8] H. Scharfetter, R. Merwa, and K. Pilz. 2005. A New Type Of Gradiometer For The Receiving Circuit Of Magnetic Induction Tomography (MIT). *Physiol. Meas.* 26(2): 307-318.

[9] B. U. Karbeyaz and N. G. Gençer. 2003. Electrical Conductivity Imaging Via Contactless Measurements: An Experimental Study. *IEEE Trans. Med. Imaging*. 22(5): 627-35.

[10] Z. Zakaria, I. Balkhis, S. Yaacob, M. S. B. Mansor, R. A. Rahim, and H. A. Rahim. 2013. Evaluation on the Sensitivity of Tri-Coil Sensor Jig for 3D Image Reconstruction in Magnetic Induction Tomography. *2013 UKSim 15th Int. Conf. Comput. Model. Simul*. 768-773.

[11] Z. Zakaria, M. Saiful, B. Mansor, R. Abdul, I. Balkhis, M. Hafiz, and F. Rahiman. 2013. Magnetic Induction Tomography: Receiver Circuit and Its Design Criteria. *J. Teknol.* 64(5): 83-87.